

A HIGH-TEMPERATURE POLYMER ELECTROLYTE MEMBRANE FUEL CELL INTEGRATED WITH A PACKED BED MEMBRANE REACTOR

P. Ribeirinha¹, T. Lagarteira¹, J. Sousa^{1,2}, A. Mendes^{1,*}

¹ Laboratório de Engenharia de Processos, Ambiente, Biotecnologia e Energia (LEPABE), Faculdade de Engenharia do Porto, Rua Roberto Frias, 4200-465 Porto, Portugal

² Departamento de Química, Escola de Ciências da Vida e do Ambiente, Universidade de Trás-os-Montes e Alto Douro, Quinta de Prados, 5000-801 - Vila Real, Portugal

*Corresponding author e-mail: mendes@fe.up.pt

ABSTRACT

In this work it is described an integrated unit combining a cellular packed bed membrane reformer (PBMR-C) and a high temperature polymer electrolyte membrane fuel cell (HT-PEMFC), operating at the same temperature (473 K). This combined system allows thermal integration, increasing this way the system efficiency. The performance of the combined units depends on the permeability, selectivity, and stability of the Pd-Ag membrane at the working temperature (473 K). This self-supported Pd-Ag membrane was produced defect free by magnetron sputtering, with a thickness of 4 μm . The membrane showed an H_2/N_2 molar selectivity of ca. 2500 and a permeability of $3.45 \times 10^{-7} \text{ mol} \cdot \text{m} \cdot \text{m}^{-2} \cdot \text{s}^{-1} \cdot \text{kPa}^{-0.7}$ at 473 K. The performance of the packed bed membrane reformer was assessed, showing concentration polarization which affected the hydrogen permeability. Despite the PBMR-C/HT-PEMFC has showed a performance lower than the one obtained with a HT-PEMFC fed with pure hydrogen at the anode side, it can promote the hydrogen pumping from the retentate side and, moreover, it can promote efficient heat integration: the heat produced in the electrochemical process can be used in the methanol steam reforming reaction.

Keywords: Fuel Cells, Pd-Ag Membrane, Methanol Steam Reforming, System Integration.

1. INTRODUCTION

High temperature polymer electrolyte membrane fuel cells (HT-PEMFCs) operate at temperatures between 393 K and 453 K and can be directly fed with methanol reformat stream (Wang *et al.*, 1996). The heat released by a HT-PEMFC is ca. 50 % of the input chemical energy, representing more energy than the necessary heat for fuel heating, vaporization and reforming reaction, all combined. Due to the mismatch on the operating temperatures between the reformer (ca. 533 K) and the HT-PEMFC, the heat released by the HT-PEMFC is mostly wasted. Designing a HT-PEMFC system incorporating fuel reformers requires special attention to the high temperatures, proper heat integration and control strategies in order to obtain a reliable, compact and efficient device (Li *et al.*, 2016). Many of these concerns could be disregarded by incorporating the methanol steam reforming (MSR) catalyst into the anodic compartment of the HT-PEMFC (internal reforming) as suggested by Avgouropoulos *et al.*, 2011.

Palladium membranes show high selectivity and high permeability to hydrogen in the range 523 K – 873 K (Iulianelli *et al.*, 2014). The introduction of a second metal such as silver to produce an alloy decreases the hydrogen diffusivity in membranes but increases the hydrogen solubility; the maximum permeability of Pd-Ag membranes to hydrogen was found for a silver content of ca. 23 wt. % [Lu *et al.*, 2007]. SINTEF developed one of the most remarkable procedures to prepare self-supported and ultrathin Pd-alloy membranes using a two-steps sputtering technique (Klette *et al.*, 2000). First the Pd-Ag film is prepared as a foil by DC-magnetron sputtering on a silicon mono-crystalline wafer used as substrate and then the metallic foil is pulled off and transferred to the testing unit.

In this work a novel packed bed membrane reactor cell (PBMR-C) coupled with a HT-PEMFC, was suggested for the first time and studied experimentally. The methanol steam reforming (MSR) catalyst was inserted in a serpentine channel of the cellular reformer, separated from the membrane electrode assembly (MEA) of the fuel cell by highly permeable and selective Pd-Ag membrane with a few microns thickness ($< 5 \mu\text{m}$). This approach, besides performing the hydrogen purification, may increase the methanol conversion, allowing the reaction to be conducted at lower temperatures, ca. 453 - 473 K. The advantages and limitations of the combined PBMR-C/HT-PEMFC unit will be discussed based on the experimental results.

2. EXPERIMENTAL

2.1. Pd-Ag membrane preparation and characterization

Palladium-silver membranes were produced by magnetron sputtering deposition (QPrep400 from Mantis Deposition®). The sputtered films were deposited onto smooth thermally oxidized silicon wafer

(Microchemicals GmbH) with 101.5 mm diameter at room temperature in a static deposition. The coated wafers were scored at the edge of the wafer and peeled out as free-standing membranes.

In order to determine the thickness of the membrane and to evaluate the membrane quality, the film was characterized by field emission scanning electron microscopy (SEM).

The permeability of the Pd-Ag membrane (4 μm thickness) was assessed using a microchannel device made of polished 316 stainless steel golden plated (Fig. 1). The membrane was placed between the feed microchannel plate (Fig. 1a) and the perforated plate (Fig. 1b). The feed microchannel plate consists on a single serpentine channel with an inlet and outlet to feed and collect the retentate gas stream, respectively.

The perforated plate (Fig. 1b) was designed to provide mechanical support to the membrane and comprehends 182 holes of 1.0 mm in diameter with a total area of 1.43 cm^2 . The permeate microchannel plate (Fig. 1c) has a double serpentine channel geometry with two outlets to collect the permeate gas. The cell was tightened using 8 bolts with a torque of 3.5 N·m. No gasket was used for sealing. The membranes in the microchannel testing device were placed in an oven and heated to the target temperature in an inert atmosphere of N_2 , before H_2 has been fed. The feed gas flow and pressure was controlled by a pressure flow meter (HORIBA STEC UR-Z712M-B). The permeated hydrogen flow was measured using a high precision film flow meter (HORIBA STEC SF) with two volumetric measuring ranges: 0.2 – 10 $\text{cm}^3\cdot\text{min}^{-1}$ (Film Flow Meter VP-1U) and 20 – 1000 $\text{cm}^3\cdot\text{min}^{-1}$ (Film Flow Meter VP-3U). During the experiments, no sweep gas was used, only the total pressure was changed.

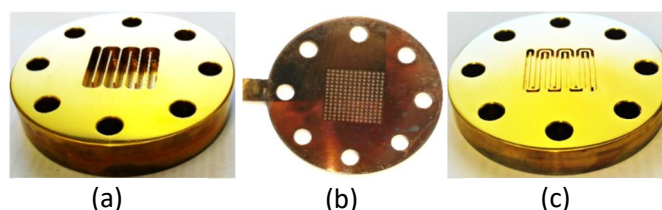


Fig. 1. Membrane testing cell. Feed microchannel plate (a), Perforated plate (b) and Permeate microchannel plate (c).

2.2. Assembly and characterization of the PBMR

The feed microchannel plate (Fig. 1a) was filled with ca. 3 g of catalyst (RP-60, BASF) with particle size in the range 200-400 μm . The Pd-Ag membrane was then placed between the feed microchannel plate (Fig. 1a) and the perforated plate (Fig. 1b). The permeate microchannel plate (Fig. 1c) was placed on the top and the device was tightened using 8 bolts with a torque of 3.5 N·m. No gasket was used for sealing. The device was placed in an oven and heated to 473 K in inert atmosphere of N_2 , before H_2 has been fed to reduce the MSR catalyst. The water/methanol liquid feed, with a steam to carbon (S/C) molar ratio of 1.5, was delivered to the PBMR using an HPLC pump (Knaur Smartline 1050). The operating pressure on the retentate side was 300 kPa. The permeate side was at the atmospheric pressure and no sweep gas was used.

2.3. HT-PEMFC characterization

The PBI membrane Fumapem® AP-40, from Fumatech, with 40 μm of thickness, was doped at 120 $^{\circ}\text{C}$ with phosphoric acid (85 %) during 3 h. The MEA was prepared using two electrodes of 5 cm^2 with a platinum loading of 1.0 $\text{mg}\cdot\text{cm}^{-2}$ and 20 wt % Pt/Carbon without Nafion®. The MEA was tested using a 5 cm^2 single cell unit from ElectroChem, Inc. Polarization curves were obtained galvanostatically between 0.05 $\text{A}\cdot\text{cm}^{-2}$ and 0.8 $\text{A}\cdot\text{cm}^{-2}$. Electrochemical impedance spectroscopy (EIS) spectra were obtained between 100 kHz and 100 mHz, with a perturbation amplitude of 5 mV. During the characterization experiments, it was used pure hydrogen as fuel in the anode and air in the cathode.

2.4. PBMR + HT-PEMFC characterization

The hydrogen produced in the PBMR (retentate side) was fed to the HT-PEMFC. The experiments were performed at 473 K, with both devices operated independently, as sketched in Fig. 2a. Polarization curves were obtained galvanostatically between 0.05 $\text{A}\cdot\text{cm}^{-2}$ and 0.2 $\text{A}\cdot\text{cm}^{-2}$. Electrochemical impedance spectroscopy (EIS) spectra were also performed.

2.5. PBMR-C/HT-PEMFC characterization

The feed microchannel plate (Fig. 1a) was filled with ca. 3 g of catalyst (RP-60, BASF) with a particle size in the range 200-400 μm . Over the feed microchannel plate (Fig. 1a), the 4 μm thickness Pd-Ag membrane was placed, followed by a gasket of ca. 200 μm thickness, the MEA, another gasket of ca. 200 μm thickness and, on the top, the permeate microchannel plate (Fig. 1c), as sketched in Fig. 2b. The device was tightened using 8 bolts with a torque of 3.5 N·m. The experiments were performed at 473 K and the pressure on the retentate side was set to 150 kPa, to avoid leakages.

Polarization curves were obtained galvanostatically between 0.05 A·cm⁻² and 0.6 A·cm⁻². Electrochemical impedance spectroscopy (EIS) spectra were obtained between 100 kHz and 100 mHz, with a perturbation amplitude of 5 mV.

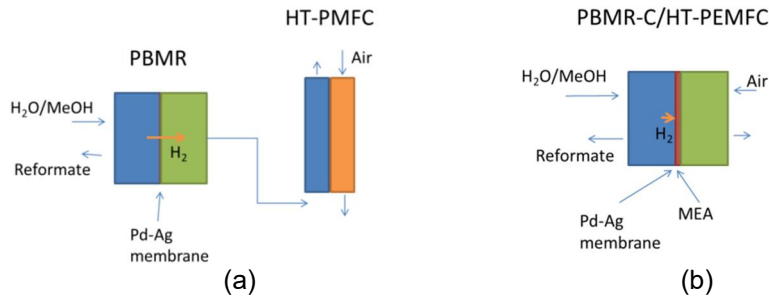


Fig. 2. Scheme of the setup considering the PBMR producing purified hydrogen to feed HT-PEMFC (a); scheme of the PBMR integrated with a HT-PEMFC (b)

3. RESULTS AND DISCUSSION

3.1 Pd-Ag membrane permeability

The membrane permeability was obtained at 473 K. At constant temperature, the hydrogen permeation flux is given by:

$$J_i = \frac{P_e}{\delta} \left(p_{i,Ret}^{\frac{1}{n}} - p_{i,Perm}^{\frac{1}{n}} \right) \quad (1)$$

where J_i is the molar flux of species i , P_e is the membrane permeability, δ is the membrane thickness and $p_{i,Ret}$ and $p_{i,Perm}$ are the partial pressure in the retentate and permeate sides, respectively. The n -value is a parameter related with the controlling step of the transport process through the membrane. For thick membranes ($>10 \mu\text{m}$), the permeation rate is limited by the hydrogen diffusion through the bulk of the membrane (Kim *et al.*, 2016), assuming an $n=2$ (Sieverts-Fick law). For thinner and thinner membranes, the controlling step of the transport process becomes more and more the hydrogen dissociation and recombination at the upper and lower membrane surfaces, respectively (Vicinanza *et al.*, 2015). In this work, performed at 473 K, the best fitting to the experimental results was obtained for $n=1.43$ (Fig. 3). The membrane permeability in these conditions was $3.45 \times 10^{-7} \text{ mol} \cdot \text{m} \cdot \text{m}^{-2} \cdot \text{s}^{-1} \cdot \text{kPa}^{-0.7}$. The selectivity was determined considering pure nitrogen in the retentate side and measuring the permeated flow rate using a high precision film flow meter (range 0.2-10 cm³·min⁻¹). At 473 K and for a feed pressure of 3 bar, no permeated nitrogen was detected, resulting in a selectivity >2500 .

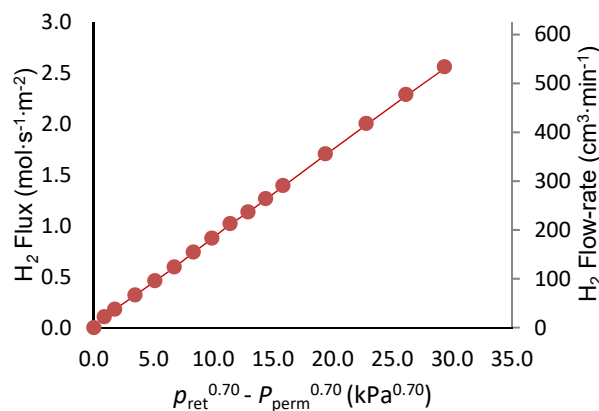


Fig. 3. Hydrogen flux and flow rate through the membrane as a function of the difference of partial pressures between retentate and permeate sides with $n=1.43$ (no sweep gas) at 473 K.

Fig. 4 shows the experimental results for the hydrogen flow rate (permeate side) as a function of the partial pressure difference between retentate and permeate sides with $n=1.43$, using a 1:1 H₂:N₂ mixture with a flow rate of 200 cm³·min⁻¹. No sweep gas was used. The low permeation may be due to the concentration polarization, that is, the faster hydrogen transport through the membrane than through the polarization gas layer (Mulder *et al.*, 1996).

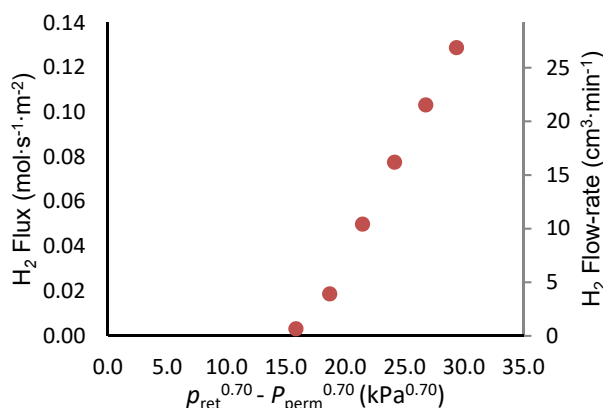


Fig. 4. Hydrogen flux and flow rate through the membrane as a function of the partial pressure difference between retentate and permeate sides. $n=1.43$, no sweep gas, $T=473$ K, 1:1 $H_2:N_2$ mixture, feed flow rate of $200 \text{ cm}^3 \cdot \text{min}^{-1}$.

3.2 PBMR performance

At 473 K, the methanol conversion is complete for a space time ratio (m_{cat}/F_{MeOH}) above $300 \text{ kg} \cdot \text{s} \cdot \text{mol}^{-1}$ (Ribeirinha *et al.*, 2018). Fig. 5 shows the experimental results for the hydrogen flow rate (permeate side) as a function of the m_{cat}/F_{MeOH} using a $H_2O/MeOH$ mixture with a steam to carbon ration (S/C) of 1.5 and a pressure of 300 kPa on the retentate side. No sweep gas was used.

Maximum hydrogen permeation is found at m_{cat}/F_{MeOH} of ca. $300 \text{ kg} \cdot \text{mol}^{-1} \cdot \text{s}$. Small m_{cat}/F_{MeOH} (high $H_2O/MeOH$ flow rates) results in low methanol conversions and consequently low hydrogen concentration. High m_{cat}/F_{MeOH} (low $H_2O/MeOH$ flow rates) results in high methanol conversions and consequently high hydrogen concentration, but low hydrogen flowrate. The concentration polarization affects severely the hydrogen permeation, due to low concentration of this component in most of the regions of the PBMR (Mulder *et al.*, 1996).

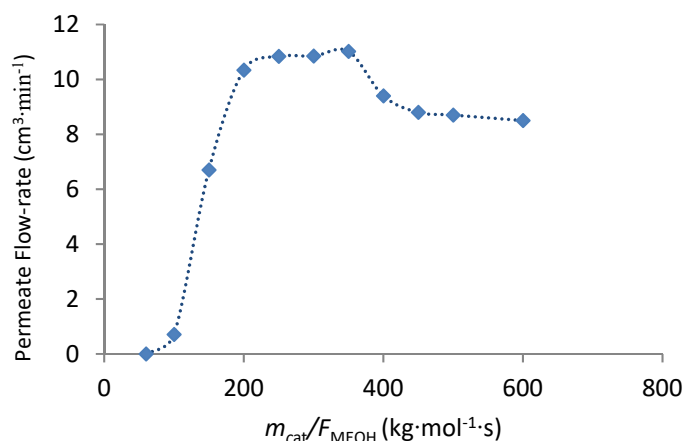


Fig. 5. Hydrogen flow rate as a function of the space time ratio (m_{cat}/F_{MeOH}) using a $H_2O/MeOH$ mixture with a steam to carbon ration (S/C) of 1.5 and a pressure of 300 kPa on the retentate side. No sweep gas was used.

After the experiments with $H_2O/MeOH$, the hydrogen permeability was assessed again using pure hydrogen in the retentate side (Fig. 6). The results show a severe drop in the hydrogen permeation, for a retentate pressure of 300 kPa: the hydrogen permeation dropped from ca. $500 \text{ cm}^3 \cdot \text{min}^{-1}$ to ca. $250 \text{ cm}^3 \cdot \text{min}^{-1}$. These results indicate that the Pd-Ag membrane was poisoned by the presence of water and methanol as reported in the literature (Israni *et al.*, 2010).

3.3 PBMR + HT-PEMFC characterization

Fig. 7 shows the polarization curves with reformat purified by the PBMR and hydrogen directly feed to the fuel cell. It is clear that the PBMR in this configuration cannot provide enough hydrogen to feed the HT-PEMFC, leading the fuel cell to starvation even at low current densities.

It is not expected the presence of contaminants (carbon monoxide, carbon dioxide and unreacted methanol or water) on the fuel, since the Pd-Ag presents a H_2 selectivity above 2500.

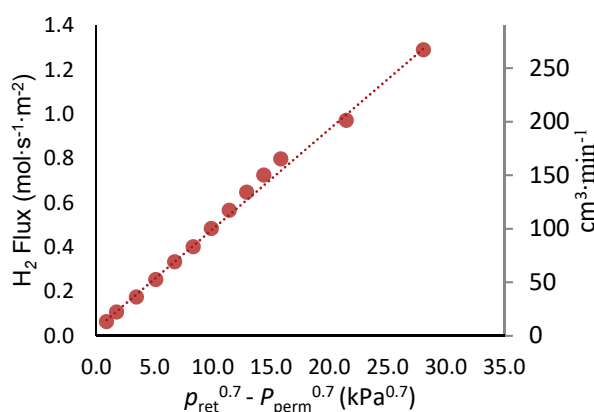


Fig. 6. Hydrogen flux and flow rate through the membrane as a function of the difference of partial pressures between retentate and permeate sides with $n=1.43$ (no sweep gas) at 473 K after permeation experiments using $H_2O/MeOH$.

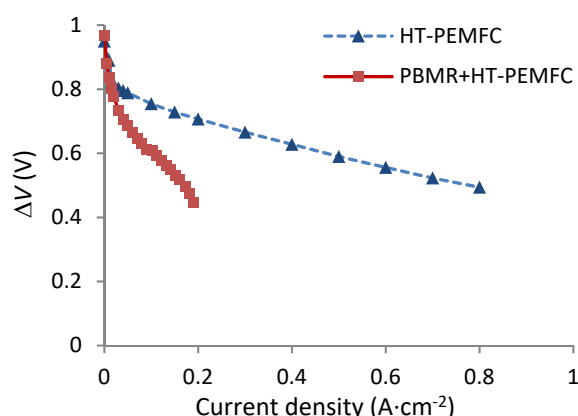


Fig. 7. Electric potential as function of the current density at 473 K, using pure hydrogen and methanol reformat. The PBMR was operated at 300 kPa and a m_{cat}/F_{MeOH} of $300 \text{ kg} \cdot \text{mol}^{-1} \cdot \text{s}$

3.4 PBMR/HT-PEMFC characterization

Fig. 8 shows the polarization curves of the HT-PEMFC fed with pure hydrogen and the polarization curves of the PBMR-C/HT-PEMFC using different m_{cat}/F_{MeOH} . The PBMR-C/HT-PEMFC unit showed lower performance than a HT-PEMFC fed with hydrogen; nevertheless, it was much higher than having both devices separated (Fig. 7). This result indicates that the hydrogen permeation through the Pg-Ag membrane was enhanced by the fuel cell – hydrogen pumping.

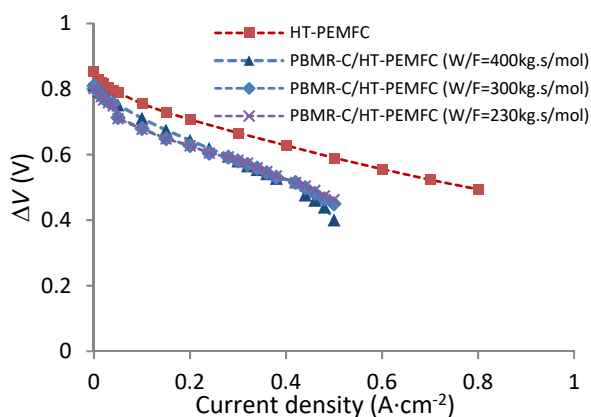


Fig. 8. Electric potential as a function of the current density at 473 K, using pure hydrogen and methanol reformat. The PBMR was operated at 150 kPa.

4. CONCLUSIONS

An integrated unit, comprising a Pd-Ag membrane reactor (PBMR-C) and a HT-PEMFC, was experimentally studied. 4 μm thick Pd-Ag membranes were prepared by magnetron sputtering. The membranes showed a hydrogen permeability of $3.45 \times 10^{-7} \text{ mol} \cdot \text{m} \cdot \text{m}^{-2} \cdot \text{s}^{-1} \cdot \text{kPa}^{-0.7}$ and selectivity above 2500. The integrated PBMR-C/HT-PEMFC unit showed higher performance than having both units operating separately. This observation indicates that the HT-PEMFC, in the integrated configuration, can promote the hydrogen pumping from the retentate side to the anode. Moreover, the PBMR-C/HT-PEMFC can promote the efficient heat integration, where the heat produced in the electrochemical process may be used by the methanol steam reformer. The lower performance of the integrated unit compared to the one obtained with a HT-PEMFC fed with pure hydrogen, was due to the polarization of the concentration in the PBMR, which affected the hydrogen permeability. Nevertheless, the high selectivity of the Pd-Ag membrane can avoid poisoning the MEA by contaminants such as methanol and/or CO.

Acknowledgments

This work was partially supported by the Projects POCI-01-0145-FEDER-006939 (Laboratory for Process Engineering, Environment, Biotechnology and Energy – UID/EQU/00511/2013) funded by the European Regional Development Fund (ERDF), through COMPETE2020 - Programa Operacional Competitividade e Internacionalização (POCI) and by national funds, through FCT - Fundação para a Ciência e a Tecnologia and NORTE-01-0145-FEDER-000005 – LEPABE-2-ECO-INNOVATION, supported by North Portugal Regional Operational Programme (NORTE 2020), under the Portugal 2020 Partnership Agreement, through the European Regional Development Fund (ERDF).

REFERENCES

- Avgouropoulos, G., Ioannides, T., Kallitsis, J. K., & Neophytides, S. (2011). Development of an internal reforming alcohol fuel cell: Concept, challenges and opportunities. *Chemical Engineering Journal*, 176, 95-101.
- Julianelli, A., Ribeirinha, P., Mendes, A., & Basile, A. (2014). Methanol steam reforming for hydrogen generation via conventional and membrane reactors: A review. *Renewable and Sustainable Energy Reviews*, 29, 355–368.
- Israni, S. H., & Harold, M. P. (2010). Methanol steam reforming in Pd-Ag membrane reactors: Effects of reaction system species on transmembrane hydrogen flux. *Ind. Eng. Chem. Res.*, 49, 10242–10250.
- Kim, C. H., Han, J. Y., Kim, N. C., Ryi, S. K., & Kim, D. W. (2016). Characteristics of dense palladium alloy membranes formed by nano-scale nucleation and lateral growth. *Journal of Membrane Science*, 502, 57–64.
- Li, Q., Aili, D., Hjuler, H. A., & Jensen, J. O. (2016). *High temperature polymer electrolyte membrane fuel cells*. Springer, Switzerland, 459-484.
- Lu, G. Q., Diniz da Costa, J. C., Duke, M., Giessler, S., Socolow, R., Williams, R. H., & Kreutz, T., (2007). Inorganic membranes for hydrogen production and purification: A critical review and perspective, *Journal of Colloid and Interface Science*, 314, 589–603.
- Mulder, M. (1996, 2nd ed.). *Basic principles of membrane technology*. Kluwer Academic Publishers, Netherlands.
- Ribeirinha, P., Mateos-Pedrero, C., Boaventura, M., Sousa, J., & Mendes, A. (2018). CuO/ZnO/Ga₂O₃ catalyst for low temperature MSR reaction: Synthesis, characterization and kinetic model. *Applied Catalysis B: Environmental*, 221, 371-379.
- Vicinanza, N., Svenum, I. H., Næss, L. N., Peters, T. A., Bredesen, R., Borg, A., & Venvik, H. J. (2015). Thickness dependent effects of solubility and surface phenomena on the hydrogen transport properties of sputtered Pd₇₇%Ag₂₃% thin film membranes. *Journal of Membrane Science*, 476, 602–608
- Wang, J. T., Savinell, R. F., Wainright, J., Litt, M., & Yu, H. (1996). A H₂/O₂ fuel cell using acid doped polybenzimidazole as polymer electrolyte. *Electrochimica Acta*, 41, 193–197.